ELSEVIER

Journal of Nuclear Materials 241–243 (1997) 842–847

journal of nuclear materials

Radial profiles of atomic deuterium measured in the boundary of TEXTOR 94 with laser-induced fluorescence

Ph. Mertens [a,*], M. Silz [b]

[a] *I.P.P., Forschungszentrum Jülich GmbH, Association EURATOM-KFA, D-52425 Jülich, Germany*
[b] *Universität GH Essen, D-45117 Essen, Germany*

Abstract

The density profiles of atomic deuterium have been recorded in the boundary plasma of TEXTOR 94 during Ohmic discharges for central, line-averaged electron densities between 1.5×10^{19} and 3.5×10^{19} m^{-3}. They have been measured in the outer equatorial plane, from the liner inwards to a few cm within the last closed flux surface, with laser-induced fluorescence at L_α (121.5 nm). The drop in density around the separatrix indicates a shorter decay length than derived from H_α-measurements in front of a limiter. The corresponding spectral profiles show the substantial contribution of a very cold component around 0.5 eV and below.

Keywords: Boundary plasma; Neutral particle diagnostic; Laser-induced fluorescence; Hydrogen; TEXTOR 94

1. Introduction

The density of a magnetically confined plasma, as produced in a tokamak [1], is sustained by the recycling of the plasma particles at the wall and limiters or divertor elements. For the understanding of the physical processes connected with the recycling, namely the neutralization, reflection, adsorption and desorption of particles at solid surfaces [2], the knowledge of the density, of the velocity distribution and of the flux is essential. As the fuel for a fusion reactor, the H-atoms and H_2-molecules and their isotopes are probably the most significant of all the recycling particles. In the past, most of the information on the densities, velocities and fluxes of atomic hydrogen was obtained from the emission intensity and from the profile of the H_α spectral line.

Detailed radiative collisional models for excitation and ionization by electron impact have been used to derive from intensities the atomic fluxes as a function of electron density n_e and temperature T_e [3]. They assume that hydrogen leaves the wall in the atomic state. However, there is experimental evidence, especially from H_α-measurements, that a substantial part of the hydrogen leaves the wall in molecular form [4]. Besides, the Doppler-broadened Balmer-profiles are not exactly representative of the velocity distribution of the hydrogen atoms, but only of those in the $n = 3$ quantum state. Thus, the further complication in emission spectroscopy arises that observed atoms are not only excited from the ground state, but also the products of dissociative excitation. Moreover, the emission spectroscopy integrates signals over the line of sight, an inherent hurdle in determining local values.

These difficulties can be circumvented when laser-induced fluorescence is used for the detection of atomic hydrogen, although at the price of a more complex experimental arrangement. Illumination with L_α radiation excites the H-atoms only. As shown in previous experiments, the power of the third harmonic of a tunable, pulsed dye laser, produced in a phase-matched mixture of argon and krypton, is sufficient for the detection of hydrogen or deuterium atoms down to about 10^{13} m^{-3} in the laboratory [5]. The same applies to a middle-sized tokamak for densities around 10^{15} m^{-3} and an energy of several eV as expected in the boundary layer: it was demonstrated a few years ago in experiments carried out in the boundary layer of TEXTOR [6] in spite of the high background radiation, but at some expense of the spatial resolution since the

* Corresponding author. Tel.: +49-2461 615 720; fax: +49-2461 613 331; e-mail: mertens@ipp880.ipp.kfa-juelich.de.

0022-3115/97/$17.00 Copyright © 1997 Elsevier Science B.V. All rights reserved.
PII S0022-3115(96)00617-4

fluorescence volume extended over about 8 cm. We describe here the first systematic investigations of the radial density profiles in the equatorial plane of the tokamak using laser-induced fluorescence, the radial resolution of 10 mm being achieved with an observation system which is perpendicular to the direction of the exciting laser. Spectral profiles can be recorded too, at any radial position.

Measurements of density profiles of atomic hydrogen with laser diagnostics were only performed on smaller tokamaks up to now. For instance, laser-induced fluorescence was applied at H_α on Unitor [7]; more recently on FT-1, the laser was used to ionize upper levels, the depletion of which was observed [8]. In both cases, the profiles could be obtained over the whole torus cross-section, but they relied, sometimes heavily, on modelling for the evaluation of the corresponding neutral density. On the opposite, we intend to use our data, measured independently of the local plasma parameters, for the purpose of model validation.

2. Principles

Laser-induced fluorescence (LIF) at L_α requires as high a power as possible at 121.534 nm (we discuss here measurements on deuterium unless otherwise specified). We improved on the system described in [5], which is primarily based on a tripling cell in an argon–krypton mixture [9]. Another possible scheme, the Raman-shifting of a frequency-doubled laser was considered in [10], but the available power and reproducibility were somewhat lower than in the case of frequency tripling. In contrast to most LIF experiments, the spectral power density of the radiation used here for L_α-excitation is below the value needed for saturation i.e. induced emission can be neglected. The fluorescence radiation is then proportional to the atomic density, to the third harmonic power available for excitation and to the cross-section for resonance fluorescence [11]:

$$\sigma_F = \pi r_e \lambda_0^2 f L(\lambda - \lambda_0) \qquad (1)$$

where r_e is the classical electron radius, λ_0 the wavelength of the atom at rest, f the oscillator strength and L the normalized line shape function. The atomic velocity v is derived from the wavelength shift. An horizontal laser polarization was achieved with a half-wave retardation plate, so that we could optimize the geometry with respect to the Zeeman effect by exciting selectively the π-components, the fine structure of which lies around 0.5 pm, a negligible effect in the interpretation of the recorded line profiles with widths around 5 pm. These values can be compared with the actual laser width, which routinely amounts to 1.4 pm at most (less than 0.7 pm with a carefully adjusted etalon). The signals can be calibrated into an absolute density scale by comparison with those from Rayleigh scattering in argon ($\sigma_R = 5.4 \times 10^{-28}$ m^2 according to [12]).

More detailed accounts of the above considerations on the application of one-photon LIF in the vacuum-UV to the detection of atomic hydrogen in fusion plasmas can be found in [13–17]. Other schemes were contemplated, such as two-photon excitation [18–20] or resonant four-wave mixing [21] (an overview is given in [22]). Unfortunately, none of them could be considered so far as suited to our purpose, owing especially to the low densities of neutral hydrogen in the range 10^{14}–10^{17} m^{-3} expected in TEXTOR. However, the situation may be different for the planned measurements in front of a limiter.

3. Experimental setup

The arrangement for L_α-measurements in the laboratory was described in [5]. For the investigations on TEXTOR 94, the setup has been slightly modified, owing to the long light path of 8 m between the laser source and the tokamak port. An excimer-pumped pulsed dye laser is used, the wavelength of which can be tuned either by tilting the grating or by changing the pressure in the oscillator chamber. Only the latter method fulfils the requirement of steepness and reproducibility (tuning over the whole spectral profile within a few s, reproducibility of the order of 0.2 pm). The wavelength was calibrated by L_α-fluorescence of thermal deuterium atoms produced on a hot tungsten wire. From the laser system located in a laboratory, the light is transmitted via two plane dielectric mirrors down to the tokamak (Fig. 1). The laser beam is focussed into the tripling cell, which contains a phase-matched argon–krypton mixture. The third harmonic radiation passes through a MgF_2 exit window before reaching the tokamak chamber. A photodiode with Au-cathode can be inserted into the beam to measure the vacuum-UV power and check for efficient tripling.

The fluorescence volume is observed at 90° to the laser and to the toroidal directions, at a distance of 1.7 m, with a Cassegrainian telescope. For the sake of convenience, we chose to scan the radial position by tilting the main mirror instead of the whole arrangement, which proved to be of no consequence. The observed volume has a length and width of about 11 mm i.e. amounts to about 1.3 cm^3. No spectral filter was required so far, but we used a gated photomultiplier ($\Delta t_{PM} \approx 10$ μs), preferably with KBr-photocathode, sensitive to the background radiation of the plasma only between roughly 115 and 140 nm. We could get rid of the low frequency noise of the plasma radiation with an electrical high-pass filter at 600 kHz.

For the Ohmic shots investigated, TEXTOR [23] has a typical toroidal field of 2–2.5 T and the plasma current amounts to 340–350 kA, with a flat-top time of up to 4–5 s in its upgraded version. The filling gas was deuterium. The laser was normally operated at 10–20 Hz throughout,

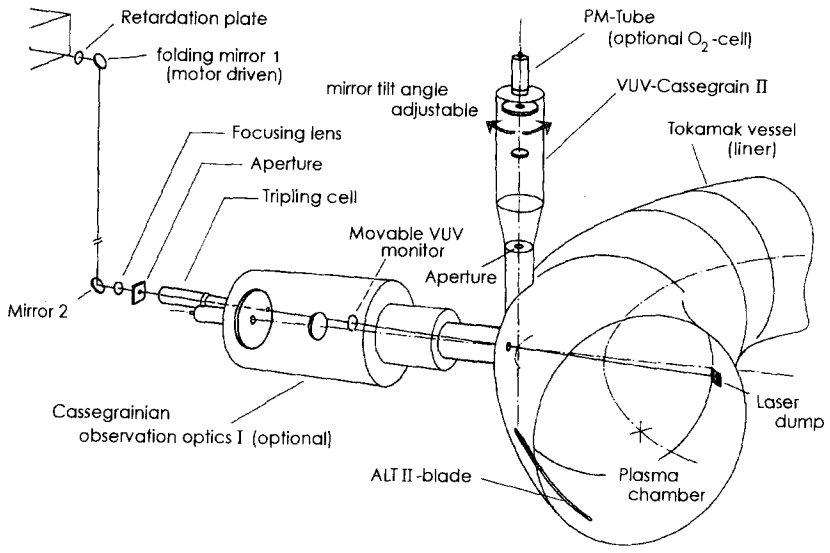

Fig. 1. Experimental setup for detection of atomic hydrogen or deuterium in the vicinity of the first wall (liner) of TEXTOR 94. The observed volume can be moved radially along the laser beam by tilting the mirror of the upper telescope. The larger equatorial telescope was not used in the present work.

which corresponds to an average drop of 38 to ≥ 30 mJ in the energy per pulse in the near UV (tripling efficiency around 10^{-4}). Fluorescence signals were simultaneously recorded by a 500 Mhz digitizer and a 'Boxcar' integrator with 12 ns gate width [24]. For each radial point, it was possible either to measure the time evolution of the density signal, or to scan the wavelength by fast pressure tuning. Beside the obvious advantage of giving spectral results within a single plasma discharge, the latter option has the drawback that, since the phase matching is usually optimized for the line centre, the exciting radiation and, consequently, the fluorescence signals are low on the wings. They can be recorded though, albeit during subsequent discharges, with a slightly shifted tripling mixture.

4. Results and discussion

Typical fluorescence signals are shown in Fig. 2 (single pulse, time evolution and pressure tuning), which presents the raw data. The S/N ratio is usually better than 15 in the centre of the line. It was better than 40 for the earlier case though (cf. [6]): the horizontal observation took advantage of a larger fluorescence volume (≥ 5 cm^3). A viewing dump is not available for the whole spatial range covered: we tilt our observation mirror inwards from the original observation dump outboard to the ALT-blade which, even when withdrawn, gives some additional background radiation. The half-width of the signals, of about 8–10 ns, is determined by the exciting pulse width (≥ 4 ns), the lifetime of the atomic level and the response time of the photomultiplier circuit.

Even at a fixed position and without spectral scanning, the L_α-fluorescence signals are of course not constant over the discharge time. The first peak, with high D^0-concentration during the startup phase, is often quite large. Later on, the signal is mainly influenced by variations in the energy per pulse of the excimer laser. To cope with the sensitivity to horizontal shifts of the plasma column, it suffices to rely on the accurate positioning obtained with the feedback of the interferometric signals of the HCN-laser (± 3 mm). A strong effect may nevertheless occur during additional heating phases, as pointed out in [25] for ICRH, depending on the condition of the first wall and on the absorption of rf-power. This will not be discussed here, since we were interested in Ohmic discharges exclusively.

Fig. 3 shows radial profiles measured from the first wall (liner at the small radius of $r = 546$ mm) in the direction of the core. Vignetting occurred for an inward tilt corresponding to $r = 465$ mm, owing to the narrowness of the cut in the liner. The amplitudes as shown in Fig. 3 are thoroughly corrected with two reference profiles: the radial density profile in a conditioning glow discharge, which is expected to be rather flat at the concerned radii [26], and the profile of the Rayleigh signals in 100 mbar argon. One should note that even at the farthest, i.e. deepest measuring point, aberrations in the imaging system are negligible with respect to our measurements [27]. As a matter of fact, it is still unclear whether the smallest radius of 445 mm corresponds to our detection limit under realistic conditions or if it can still be improved on. For all shots shown, the main poloidal limiters were positioned at 460 mm, which determines the last closed flux surface (LCFS) and all eight blades of the toroidal belt limiter ALT-II were

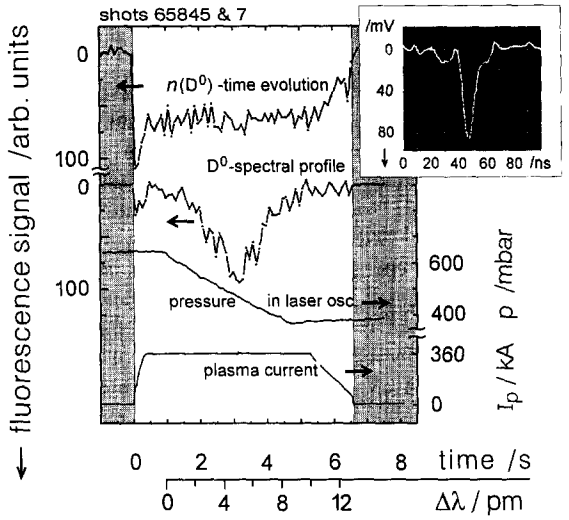

Fig. 2. Raw signals from the boxcar integrator. (a) The upper trace represents the time evolution of the density: each point corresponds to a single laser shot. (b) The second trace is a spectral profile obtained during the 4 s plateau of the tokamak discharge. (c) The third one is the pressure variation in the laser oscillator, which represents the wavelength. (d) The last signal is the plasma current. The inset shows a time-resolved fluorescence signal.

given the same radius between 460 and 468 mm. The profiles are rather flat from the wall inwards to about 1 cm outside of the LCFS. The expected drop in density around the separatrix corresponds to an estimated decrease of the atomic mean free path by roughly a factor of 10 (from a rate coefficient for the ionization by electron impact of $\langle \sigma v_e \rangle_i = 2.5\text{–}3.0 \times 10^{-8}$ cm^3/s and an electron density

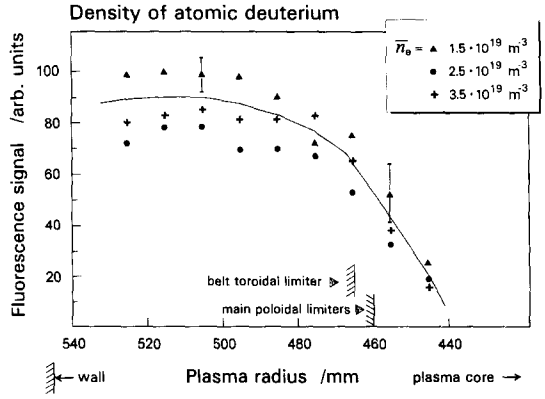

Fig. 3. Radial profiles of the atomic density from the liner, on the left side, inwards to the small radius of 445 mm. The position of the main limiters is indicated. The full scale of 100 corresponds to a density of 5×10^{15} atoms/m^3 in a velocity interval of 4×10^4 m/s (see text for explanation). Different symbols correspond to different central densities $\bar{n}_e$. The solid line is drawn only to guide the eye.

increase of 1×10^{18} to 1×10^{19} m^{-3} at most, as given by the n_e and T_e radial profiles recorded in the boundary layer by the lithium and helium beam diagnostic systems in the next toroidal section of the machine [28,29]). The amplitude of the neutral deuterium signal itself drops by a factor of about 4 within 30 mm; this value will be refined when the line of sight to the smaller radii is improved, since the last point at 445 mm is still uncertain. It indicates anyway a smaller 1/e-decay length than derived from H_α measurements in front of a limiter (cf. [30]), which is probably due to the more important role of the molecules in the present measurement. In the domain investigated, Ohmic shots with an averaged central electron density of $\bar{n}_e = 1.5$ to 3.5×10^{19} m^{-3}, the D^0-density was rather insensitive to plasma conditions: only a slight increase of at most 10% in the signal was recorded in the plateau for the step from 2.5 to 3.5×10^{19} m^{-3}. It is still unclear why the profiles corresponding to the lowest central density lie slightly above the other ones; it might indeed be accounted for by a very successful toroidal adjustment and by somewhat different plasma conditions for this series of measurements.

Fig. 4 shows the spectral profiles at two different radial positions. Both are indeed a bit narrower than recorded before with an horizontal observation system [6]. This is not surprising since we are not integrating any more over the whole depth of the outer boundary layer. The profiles correspond to velocity distributions along the laser beam, which are not Gaussian. They look somewhat more sym-

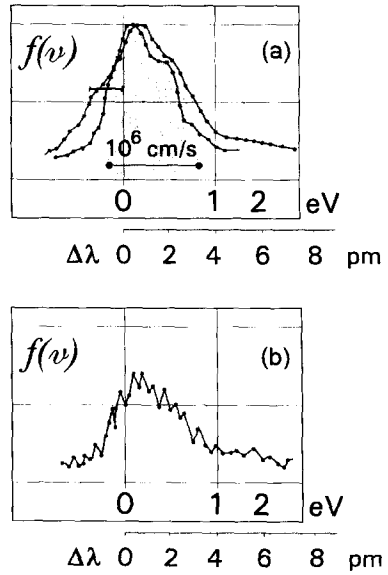

Fig. 4. Velocity distributions of atomic deuterium at two different radii: (a) 500 mm and (b) 470 mm. The curves in (a) were recorded on different days, showing the maximal uncertainty on the position relatively to the reference wavelength. The (b) curve shows a lower S/N-ratio but a comparable width to the first ones.

metrical than before, but the near-wings further indicate low temperatures (0.2–1.7 eV). Further away from the reference wavelength, the wings decay much slower than Gaussian profiles, in fact a signal is still detectable around 5 eV if the gas mixture in the tripling cell is changed to match the corresponding wavelength. On the other side, the predominance of particles below 1 eV, even just below 0.5 eV comes up distinctly. Several processes involving molecular dissociation can account for these low energies per atom [31,32], for instance electron-impact dissociations of the type:

$$H_2 + e \rightarrow H(1s) + H^*(n=3) + e$$

$$H_2 + e \rightarrow H(1s) + H^*(2s) + e$$

$$H_2^+ + e \rightarrow H^+ + H(1s) + e. \qquad (2)$$

These processes and accordingly the molecules are privileged candidates as a source for the detected atoms in the boundary layer, especially with the slight spectral asymmetry called to mind hereabove. Apart from the obvious loss in S/N ratio, the spectral profiles at different radial positions in the outer boundary layer are quite similar, which is not surprising in view of their supposed molecular origin and mean free path. However, the spectral profiles within the separatrix, for instance at $r = 445$ mm, appear somewhat broader than those which are measured outside. Due to the above-mentioned technical hitch, they could not yet be recorded satisfactorily.

At this stage, it is worth mentioning that other measurements were performed at the Balmer α–γ lines in emission spectroscopy, for similar or even in some cases for the very same shots, around $r = 470$ mm [33]. Although they may correspond to different dissociation processes with excitation of the $n = 3$ level, they also give a clue to the importance of the molecular origin, to the presence of a substantial contribution of a very cold component around 0.5 eV and below and to the insensitiveness to the core plasma conditions in Ohmic regime. The unexpectedly cold component to the atomic velocity distribution is attributed to electron impact-induced dissociation, precisely dissociative excitation, which holds true for a wide range of plasma conditions.

A density calibration by comparison with the signals from Rayleigh scattering was attempted in 0–100 mbar argon. A signal to noise ratio of at least 5 was obtained from 50 mbar on. Careful filling is required to avoid the introduction of water ($\sigma_{Abs} \approx 1.5 \times 10^{-21}$ m^2). The calibration confirmed the previous attempt with the older observation system and gave around $r = 500$ mm a density of about 5×10^{15} m^{-3} within a velocity interval of 10^4 m/s, which covers the main part of the distribution. The total density could actually be a factor of two higher if one considers a broader spectral range than scanned during single plasma discharges (we covered the energy range 0–6 eV and left higher energies for future investigations).

5. Conclusions and prospects

It has been shown that laser-induced fluorescence in the vacuum-UV can be used to determine the atomic density of hydrogen — in the present case deuterium — near the wall of a tokamak of the size of TEXTOR 94. The Lyman-alpha line is indeed helpful in measuring densities below 10^{18} m^{-3} and the corresponding velocity distributions in the low energy range. Radial profiles are found to be fairly flat in the outer boundary layer and to decay rather fast around the radius of the main limiters. The spectral profiles reveal a substantial amount of atoms with energies below 1 eV, an indication of probable molecular origin. In both cases, a scan of the averaged central density of the tokamak did not show any pronounced variation. The precedence of ALT-II and the required consistence of the profiles will be taken into account more accurately when the radial range is further extended inwards (5–10 mm), especially within the frame of the EIRENE-code [34]. Here, our independent measurement could contribute in validating the model for a new configuration.

Acknowledgements

The authors pay tribute to the late Dr. P. Bogen for his decisive promoting of the concept and resolute commitment in the installation of the original diagnostic system on TEXTOR. They are also indebted to Professor E. Hintz and to Dr. U. Samm for their interest and support in the present investigations.

References

[1] H.P. Furth, The Tokamak, in: Fusion, ed. E. Teller, Vol. 1 (Academic Press, 1981).
[2] D.E. Post and R. Behrisch (eds.), Physics of Plasma-Wall-Interactions in Controlled Fusion, NATO ASI Series B, Vol. 131 (Plenum Press, 1986) pp. 1183 ff. (cf. esp. pp. 695 sqq.).
[3] L.C. Johnson and E. Hinnov, J. Quant. Spectrosc. Radiat. Transfer 13 (1973) 333–358.
[4] M.F.A. Harrison, in: Physics of Plasma-Wall-Interactions in Controlled Fusion, eds. D.E. Post and R. Behrisch, NATO ASI Series B, Vol. 131 (Plenum Press, 1986) pp. 281–349.
[5] Ph. Mertens and P. Bogen, Appl. Phys. A 43 (1987) 197–204.
[6] Ph. Mertens and P. Bogen, Proc. 16th Eur. Conf. on Controlled Fusion and Plasma Phys. 13B/III (1987) 983–986.
[7] J. Hackmann, C. Gillet, G. Reinhold, G. Ritter and J. Uhlenbusch, J. Nucl. Mater. 111–112 (1982) 221–225.
[8] V.I. Gladushchak, G.T. Razdobarin et al., Nucl. Fusion 35(11) (1995) 1385–1390.
[9] R. Mahon, T.J. McIlrath, V.P. Myerscough and D.W. Koopman, IEEE J. Quant. Electron. 15(6) (1979) 444–451.
[10] P. Bogen, Ph. Mertens, E. Pasch and H.F. Döbele, J. Opt. Soc. Am. B 9–12 (1992) 2137–2141.

[11] A. Unsöld, Physik der Sternatmosphären, Nachdruck der 2. Auflage (Springer-Verlag, 1968) pp. 866 ff.
[12] G.I. Chashchina, V.I. Gladushchak and E.Ya. Schreider, Opt. Spektrosk. 24 (1968) 1008–1010.
[13] Ph. Mertens, Rep. KFA Jülich Jül-2154, ISSN 0366–0885 (1987) 82 pp. (in German).
[14] P. Bogen, R.W. Dreyfus and Y.T. Lie, J. Nucl. Mater. 111–112 (1982) 75–80.
[15] P. Gohil and D.D. Burgess, Rep. UKAEA CLM-P679, Culham (1982) 22.
[16] P. Bogen, Jet Design Study 14.2, Rep. KFA-IPP-IB-2/83 (1984) 21.
[17] D. Voslamber, Rep. DRFC Cadarache EUR-CEA-FC-1342 (1988) 127.
[18] D. Voslamber, Rep. DRFC Cadarache EUR-CEA-FC-1387 (1990) 75.
[19] K. Grützmacher, M.I. de la Rosa and A. Steiger, Proc. 7th Symp. on Laser-Aided Plasma Diagnostics, ed. K. Muraoka, Fukuoka (1995) pp. 156–161.
[20] K. Muraoka, J. Nucl. Mater. 220–222 (1995) 563–566.
[21] U. Czarnetzki and H.F. Döbele, Rev. Sci. Instrum. 66(1) (1995) 587–589.
[22] K. Muraoka and M. Maeda, Plasma Phys. Controlled Fusion 35 (1993) 633–656.
[23] H. Soltwisch et al., Plasma Phys. Controlled Fusion 26(1A) (1984) 23–35.
[24] Tektronix 7912 AD & EG and G 4400.
[25] G. Van Oost et al., Proc. 20th Eur. Conf. on Controlled Fusion and Plasma Phys. 17C/II (1993) pp. 671–674.
[26] J. Winter, Rep. KFA Jülich Jül-2207, ISSN 0366-0885 (1988) 159 pp. (in German).
[27] D. Rusbüldt, private communication.
[28] B. Schweer et al., J. Nucl. Mater. 196–198 (1992) 174–178.
[29] E. Hintz and B. Schweer, Plasma Phys. Controlled Fusion 37 (1995) A87–A101.
[30] U. Samm et al., J. Nucl. Mater. 162–164 (1989) 24–37.
[31] R.K. Janev, W.D. Langer, K. Evans and D.E. Post, Elementary Processes in Hydrogen–Helium Plasmas (Cross Sections and Rate Coefficients), Springer Series on Atoms + Plasmas, Vol. 4 (1987) 326 pp.
[32] D. Reiter, P. Bogen and U. Samm, J. Nucl. Mater. 196–198 (1992) 1059–1064.
[33] J.D. Hey et al., Contrib. Plasma Phys. 36(5) (1996) 583.
[34] D. Reiter, Neutral Gas Transport in Fusion Devices: Atomic and Surface Data Aspects — EIRENE in Atomic and Plasma-material Interaction Processes in Controlled Thermonuclear Fusion, eds. R.K. Janev and H.W. Drawin (Elsevier, 1993) pp. 243–266.